

PROPERTIES OF HIGH-TEMPERATURE SUPERCONDUCTORS IN A TWO-BAND MODEL WITH THE DOPING-DEPENDENT ELECTRON SPECTRUM

Nikolai KRISTOFFEL and Pavel RUBIN

Institute of Physics, University of Tartu, Riia 142, 51014 Tartu, Estonia; kolja@fi.tartu.ee

Received 28 March 2001, in revised form 14 May 2001

Abstract. A simple model of interband superconductivity, incorporating a basic band and a doping created one (constant total number of states), is considered, keeping in mind the two-component scenario of high- T_c superconductivity. The dependences of T_c , its isotope exponent, superconductivity gaps, etc. on doping are calculated using an illustrative set of parameters. The observed types of behaviour are reproduced. Diminishing gap ratios with hole doping have been found. In the one-particle excitation spectrum the peak–dip–hump type complex can be identified. In spite of crude approximations the model reflects, in general, the experimental findings on high- T_c cuprates. Two-band models will remain a channel for looking for the high- T_c mechanism.

Key words: high-temperature superconductivity, two-band models, doping, gaps.

1. INTRODUCTION

The superconductivity mechanism of high- T_c cuprate systems is still under debate and a number of different theories are being developed. The present work concentrates on one of the possible approaches.

Numerous results point to the multicomponent nature of the order parameter, several elementary excitation gaps, two pairing scales, participation of several electronic bands or subsystems, etc. in the basic physics of cuprate superconductors (e.g. [1–5]). This trend is nowadays concentrated in the “two-component scenario” of high- T_c superconductivity [6–11]. It establishes the participation of two different electronic subsystems one of which is of basic itinerant, the other of quasilocalized nature, the latter being associated with the doping treatment.

These subsystems (bands) can be presumably connected with doping-induced stripe-ordering phase separation in the superconductivity playground CuO_2 planes [12–17]. This self-organization process in the two-dimensional electron subsystem generates undistorted material stripes alternating with doping charge bearing distorted regions. This charge and spin (static or fluctuating) inhomogeneity is considered as a key phenomenon in the physics of superconducting cuprates [18].

In connection with the two-component scenario a hole-type itinerant band and a narrow doping-created distribution of (localized; percolating) states are usually mentioned. It seems natural to describe the superconductivity mechanism in such a situation by two-band models [19–21]. A number of various two-band schemes have been developed using interacting partners traced back to different origins. Particularly, characteristic trends of T_c , its isotope effect exponent and some properties of gaps were obtained in the scheme of two overlapping bands in papers [21–27].

Only few recent approaches use a doping-dependent electron spectrum or connect it with striping. A multiband description of the cuprate high- T_c phenomenon on stripe-split band components was developed in [16]. A model exploiting repulsive (Coulombic plus small electron–phonon) interaction of an itinerant band with a doping-created δ -type higher lying state was considered in [27].

Recent experimental investigations have yielded more precise and partly unexpected results which need theoretical explanation. The two-component scenario has been supported by measuring the isotope effect also on the paired carrier effective mass (penetration depth), traced to polarons [10]. Further, two quasiparticle relaxation times of critical and noncritical behaviour were found [11]. In [26], the isotope effect of the supercarrier effective mass was looked for using a two-band model and the observed behaviour was revealed (see also [28]). In [29] it was shown that the presence of a critical and a noncritical relaxation channel is a natural consequence in two-band models.

Recent tunnelling experiments [30–35], in accordance with the photoemission studies [34–36], have essentially added to reproducible information on excitation spectra and gaps. The one-particle excitation spectrum exhibits a typical peak–dip–hump complex structure. It is considered as a consequence of the opening of the superconducting gap in the electron spectrum and as being of collective origin [30]. This feature is regarded as setting several constraints on theoretical models of pairing interaction [31]. Recently some theoretical attempts have been made to describe the tunnelling spectra of such type [37–40]. Most interesting is the result of [31,33] that the gap to T_c ratio $2\Delta(0)/kT_c$, and even the gap itself is, contrary to T_c , a decreasing function of doping in the “higher” part of the underdoped region. The characteristic ratios mentioned are found to be of non-BCS universality, reaching large values near 10. Theoretically the possibility of a $2\Delta(0)/\Theta_c$ ratio ($\Theta = kT$) diminishing with doping has been already demonstrated in [23].

In the present contribution we demonstrate the ability of a very simple two-band model to show the qualitative tendencies mentioned above. This model supposes repulsive interband scattering of intraband pairs between an itinerant band and a narrow distribution of states appearing and expanding with doping at the cost of the number of states of the first band. Taking account also of previous results, it seems that two-band models with doping-dependent electron energy distributions will be able to describe basic superconductivity characteristics in high- T_c cuprates. Correspondingly, such models will serve as a way to look for the high- T_c mechanism.

2. BASIC FORMULAS

We start with the linearized Hamiltonian of a two-band (a and b) superconductor with the leading interband scattering of the intraband pairs

$$\begin{aligned}
H = & \sum_{\vec{k}\sigma} \varepsilon_a(\vec{k}) a_{\vec{k}\sigma}^+ a_{\vec{k}\sigma} + \sum_{\vec{k}\sigma} \varepsilon_b(\vec{k}) b_{\vec{k}\sigma}^+ b_{\vec{k}\sigma} \\
& + \sum_{\vec{k}} \Delta_a(\vec{k}) \left[a_{\vec{k}\uparrow} a_{-\vec{k}\downarrow} + a_{-\vec{k}\downarrow}^+ a_{\vec{k}\uparrow}^+ \right] - \sum_{\vec{k}} \Delta_b(\vec{k}) \left[b_{\vec{k}\uparrow} b_{-\vec{k}\downarrow} + b_{-\vec{k}\downarrow}^+ b_{\vec{k}\uparrow}^+ \right].
\end{aligned} \tag{1}$$

The order parameters (gaps) are defined as

$$\begin{aligned}
\Delta_a(\vec{q}) &= 2 \sum_{\vec{k}} W(\vec{q}, \vec{k}) \langle b_{\vec{k}\uparrow} b_{-\vec{k}\downarrow} \rangle = 2 \sum_{\vec{k}} W(\vec{q}, \vec{k}) \langle b_{-\vec{k}\downarrow}^+ b_{\vec{k}\uparrow}^+ \rangle, \\
\Delta_b(\vec{q}) &= 2 \sum_{\vec{k}} W(\vec{q}, \vec{k}) \langle a_{-\vec{k}\downarrow} a_{\vec{k}\uparrow} \rangle = 2 \sum_{\vec{k}} W(\vec{q}, \vec{k}) \langle a_{\vec{k}\uparrow}^+ a_{-\vec{k}\downarrow}^+ \rangle.
\end{aligned} \tag{2}$$

In (1) usual designations are used. The band energies read $\xi_{a,b}(\vec{k}) = \varepsilon_{a,b}(\vec{k}) + \mu$, μ being the chemical potential. The interaction constant $W = U + V$ characterizing the interband scattering of pairs contains the Coulomb electronic (U) and the electron–phonon part (V), both of which are repulsive. The contribution of interband pairs is omitted with the usual argument of much smaller momentum scattering volume available. Diagonalization of (1) leads to the gap equations

$$\begin{aligned}
\Delta_a(\vec{q}) &= \sum_{\vec{k}} W(\vec{q}, \vec{k}) \Delta_b(\vec{k}) E_b^{-1}(\vec{k}) th \frac{E_b(\vec{k})}{2\Theta}, \\
\Delta_b(\vec{q}) &= \sum_{\vec{k}} W(\vec{q}, \vec{k}) \Delta_a(\vec{k}) E_a^{-1}(\vec{k}) th \frac{E_a(\vec{k})}{2\Theta}
\end{aligned} \tag{3}$$

with the one-particle excitation energies

$$E_{a,b}(\vec{k}) = \sqrt{\varepsilon_{a,b}^2(\vec{k}) + \Delta_{a,b}^2}. \quad (4)$$

Two-particle interband excitation energies are determined by $E_a \pm E_b$. The occupation numbers of the renormalized bands per one spin read

$$n_{a,b}(\vec{k}\sigma) = \frac{1}{2} \left[1 - \frac{\varepsilon_{a,b}(\vec{k})}{E_{a,b}(\vec{k})} \tanh \frac{E_{a,b}(\vec{k})}{2\Theta} \right]. \quad (5)$$

Supposing further that the lower band (a) is extended in energy from 0 to D with the constant density of states ρ_a (two-dimensionality of CuO_2 planes), and the higher band (b) is analogously extended from ε_1 to ε_2 , one finds, in the case of wave-vector independent W and gaps, the approximate expression ($\gamma = e^{0.577}$) for the transition temperature:

$$\Theta_c = \frac{2\gamma}{\pi} \sqrt{D(\varepsilon_2 - D)} \exp \left\{ -\frac{1}{2} \left[\ln^2 \frac{D}{\varepsilon_2 - D} + \frac{4}{\rho_a \rho_b W^2} \right]^{1/2} \right\}. \quad (6)$$

The Θ_c isotope effect exponent is found as

$$\alpha = -C \frac{V}{W} \cdot \frac{1}{W^2 \rho_a \rho_b} \left[\ln \frac{\pi}{2\gamma} \frac{\Theta_c}{\sqrt{D(\varepsilon_2 - D)}} \right]^{-1}, \quad (7)$$

where $C = d \ln M / d \ln M_i$ and M is the effective mass of the active vibration, while M_i is the atomic mass under substitution. Note that for interband interaction $V \sim M^{-1}$.

The superconductivity gaps (vanishing simultaneously at Θ_c) at zero temperature are determined from the system

$$\begin{aligned} |\Delta_a(0)| &= W \rho_b |\Delta_b(0)| \ln \frac{\sqrt{(\varepsilon_2 - D)^2 + \Delta_b(0)^2} + \varepsilon_2 - D}{|\Delta_b(0)|}, \\ |\Delta_b(0)| &= W \rho_a |\Delta_a(0)| \ln \frac{\sqrt{D^2 + \Delta_a(0)^2} + D}{|\Delta_a(0)|}. \end{aligned} \quad (8)$$

Further comments on the scheme used and approximations made can be found in [21].

3. THE MODEL AND ILLUSTRATIVE CALCULATIONS

Below we present an interpolative model to describe the two-component scenario and to consider basic dependences of superconductivity characteristics.

In quantitative illustrative calculations a reasonable nonspecified set of parameters will be used. Correspondingly, the doping will be characterized by a concentration c , which as a measure can be scaled to a real number of holes introduced into the superconductivity playground.

We suppose that with hole doping over the upper edge of the a-band filled at $c = 0$ a new distribution of electronic states (b-band) will be formed at the equalized cost of a-band states. Let the width of the b-band develop so that $\varepsilon_2 = D + \nu c^2$ and $\varepsilon_1 = D$. Then $\rho_a = D^{-1}(1 - c)$, $\rho_b = (\nu c)^{-1}$ and (with a good accuracy also for $T < T_c$) $\mu = D$. Correspondingly,

$$\Theta_c = 1.14c\sqrt{D\nu} \exp \left\{ -\frac{1}{2} \left[\frac{4\nu D}{W^2} \cdot \frac{c}{1-c} + \ln^2 \frac{D}{\nu c^2} \right]^{1/2} \right\}. \quad (9)$$

To deal with a system possessing T_c near 100 K for optimal doping, we choose the following set of parameters: $D = 3$, $\nu = 1$, $W = 0.3$ (eV).

Clearly, the use of wave-vector independent interband coupling and gaps appears as a crude supposition as compared with the established d-wave-dominating nature of the order parameter in high- T_c cuprates. However, the results obtained in the framework of the present work seem to be stimulating for further research, which must include \vec{k} -dependent characteristics connected with the doping-dependent electron spectrum that the authors are not able to introduce at the present. Such a doping dependence can be traced back to strong electronic correlations acting in cuprates.

The behaviour of superconductivity characteristics in the present model is illustrated by Figs. 1–4. The zero-temperature superconductivity gaps $\Delta_{a,b}(0)$ and the transition-temperature T_c show the usual rise on the way to optimal doping with the following decrease by overdoping (Fig. 1). In connection with the experimental findings discussed in the Introduction, it should be mentioned that the $\Delta_{a,b}(0)$ maxima are shifted to weaker dopings as compared to T_c .

The behaviour of the characteristic ratios $2\Delta_{a,b}(0)/\Theta_c$ with doping is illustrated in Fig. 2. In the case of the smaller gap (doping-induced band) this ratio diminishes smoothly with doping. This is in agreement with the experiment of [31–33]. For the other (basic) band $2\Delta_a(0)/\Theta_c$ possesses a maximum in the region of extended underdoping with the following slow change from diminishing to enhancement. The BCS universality in $2\Delta_{a,b}(0)/\Theta_c$ is violated and large values near 10 can arise as observed in numerous experiments. The $\Delta_{a,b}(T)$ dependences are of the usual form (Fig. 3).

The isotope effect exponent (Fig. 4) rises with doping and is not enhanced for underdoping because of the doping-created nature of the b-band. For the c -independent narrow band submerged in the wider one, α is enhanced for both under- and overdoped regions where T_c becomes small [21,22]. Note that a small percentage of the electron–phonon contribution to the whole interband interaction can lead to remarkable α -values.

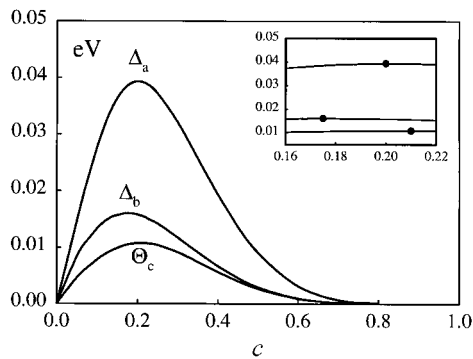


Fig. 1. The dependences of the transition temperature and zero temperature gaps on doping for an illustrative set of parameters. In the inset the maxima positions of these quantities are indicated by points.

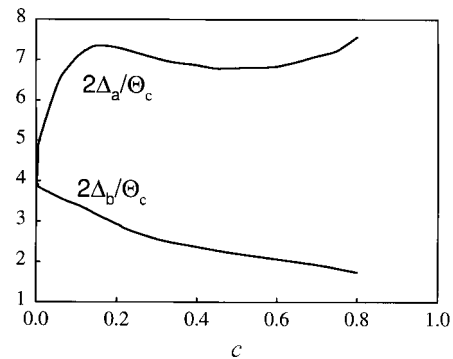


Fig. 2. Characteristic zero-temperature gap ratios as functions of doping.

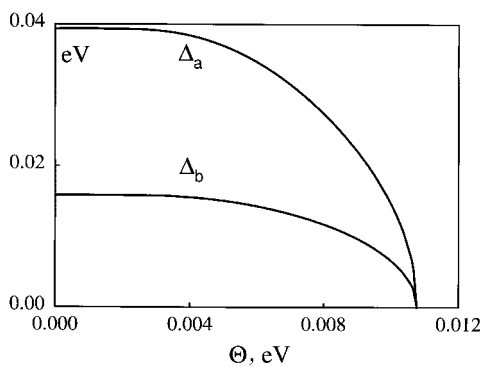


Fig. 3. The superconductivity gaps dependent on temperature, $c = 0.20$.

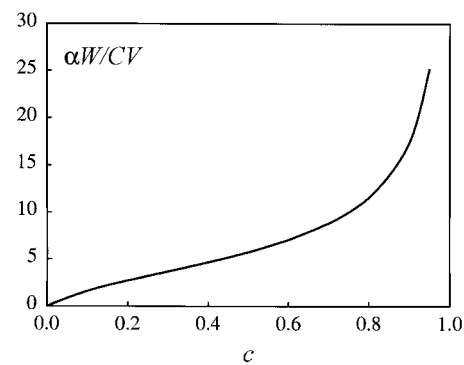


Fig. 4. Transition-temperature isotope exponent vs. doping.

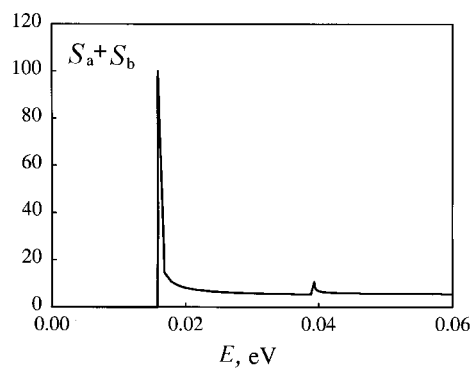


Fig. 5. Joint density of one-particle excitations, $c = 0.20$.

The one-particle densities $S_{a,b}(E) = \rho_{a,b}E[E^2 - \Delta_{a,b}^2]^{-1/2}$ calculated (without taking account of dispersion, damping, etc.) are of rough guiding nature. However, the characteristic structure of the peak–dip–hump type is recognizable ($T < T_c$) in the joint density if one associates the peak with Δ_b and the hump with Δ_a (Fig. 5). The spectral feature intensities are determined using ρ_a/ρ_b . We mention that arguments given in [36] against a two-band interpretation of the peak plus hump feature naturally fail ($\Delta_a = 0$ for $T > T_c$; interband nature of the interactions). The Δ_b behaviour is reflected by the peak. In [36] it is found that the hump shifts to greater energies with decreasing doping in underdoped samples. Our model exhibits the hump in an extended underdoped region at higher energies with lowering c . Later this behaviour converts to the opposite until the hump becomes hidden in the peak for small c . The temperature approaching T_c quenches the structure under consideration.

A remark must be made concerning the widely expressed statement that the only one Fermi surface observed introduces discrepancies with the two-band models for which two surfaces can be expected. This argument has no formal relevance for the present model because of the doping-independent position of the chemical potential at the energy where the bands touch each other ($\mu = D$). Experimentally there are indications of such a trend at least for some systems ($\text{Bi}_2\text{Sr}_2\text{CaCu}_2\text{O}_{8+\delta}$) [34,36].

Further, the observability of two Fermi surfaces is not necessarily dictated by the two bands present. For instance, according to t-J model calculations [41], the narrow and wide bands cross the Fermi surface at nearly the same \vec{k} , however, their spectral intensities differ markedly. The weaker wide band maximum becomes masked (cf. also Fig. 5 for connected results) and contributes only to the finite spectral intensity at the Fermi surface. A model using μ lowering with doping will enable also the description of the pseudogap as a natural excitation threshold of the a-band system in the underdoped region, which transforms with further doping to the usual Δ_a .

In conclusion, we note that in spite of all the crude approximations of the model discussed, it can reflect some important dependences and tendencies observed in cuprate high-temperature superconductors. Correspondingly the two-band models remain a channel in which the microscopical mechanism of the high- T_c phenomenon can be looked for.

ACKNOWLEDGEMENTS

This work was supported by the Estonian Science Foundation (grant No. 3591). One of the authors (N. K.) is indebted to T. Timusk for the comments on the experimental data.

REFERENCES

1. Kresin, V. Z. and Wolf, S. A. Multigap structure in cuprates. *Physica C*, 1990, **169**, 476–484.
2. Genzel, L., Wittlin, A., Bauer, M., Cardona, M., Schönherr, E. and Simon, A. Phonon anomalies and range of superconductivity energy gaps from infrared studies. *Phys. Rev.*, 1989, **B40**, 2170–2178.
3. Heyen, E. T., Cardona, M., Karpinski, J., Kaldis, E. and Rusiecki, E. Two superconducting gaps and electron-phonon coupling in $\text{YBa}_2\text{Cu}_3\text{O}_8$. *Phys. Rev.*, 1991, **B43**, 12958–12975.
4. Srikanth, H., Zhai, Z., Sridhan, S., Erb, A. and Walker, E. Systematics of two-component superconductivity from microwave measurements. *Phys. Rev.*, 1998, **B57**, 7986–7996.
5. Shen, Z.-X., White, P. J., Feng, D. J., Kim, C., Gu, G. D., Ikeda, H., Yoshizaki, R. and Koshizuka, N. Temperature-induced momentum-dependent spectral weight transfer in $\text{Bi}_2\text{Sr}_2\text{CaCu}_2\text{O}_{8+\delta}$. *Science*, 1998, **280**, 259–263.
6. Billinge, S. J. L. and Egami, T. Short-range atomic structure of $\text{Nd}_{2-x}\text{Ce}_x\text{CuO}_{4-y}$ determined by real-space refinement at neutron-powder-diffraction data. *Phys. Rev.*, 1993, **B47**, 14386–14406.
7. Mihailović, D., Mertelj, T., Podobnik, B., Demsar, J., Canfield, P., Fisk, Z. and Chen, C. Evidence for polaronic states in metallic $\text{YBa}_2\text{Cu}_3\text{O}_{6.9}$ from ultrafast phonon Raman spectroscopy. *Physica B*, 1996, **219/220**, 142–144.
8. Stevens, C. J., Smith, D., Chen, C., Ryan, J. F., Podobnik, B., Mihailović, D., Wagner, G. A. and Evetts, J. E. Evidence for two-component high- T_c superconductivity in the femtosecond optical response. *Phys. Rev. Lett.*, 1997, **78**, 2212–2216.
9. Mihailović, D. and Müller, K. A. The two-component paradigm for superconductivity in the cuprates. In *Proc. NATO ASI Materials Aspects of High- T_c Superconductivity*. Kluwer, Dordrecht, 1997, 1–14.
10. Zhao, G., Conder, K., Keller, H. and Müller, K. A. Oxygen isotope effects in $\text{La}_{2-x}\text{Sr}_x\text{CuO}_4$: evidence for polaronic charge carriers and their conduction. *J. Phys. Condens. Matter*, 1998, **10**, 9055–9066.
11. Demsar, J., Podobnik, B., Kabanov, V. V., Wolf, Th. and Mihailović, D. Superconducting gaps, the pseudogap and pair fluctuations above T_c . *Phys. Rev. Lett.*, 1999, **82**, 4918–4921.
12. Salkoda, M. J., Emery, V. J. and Kivelson, S. A. Metallic stripes in high- T_c superconductor. *J. Supercond.*, 1996, **9**, 401–406.
13. Egami, T. Electron–lattice interaction in cuprates. *J. Low Temp.*, 1996, **105**, 791–800.
14. Bianconi, A., Saini, N. L., Rossetti, T., Lanzara, A., Perali, A., Missori, M., Oyanagi, H., Yamaguchi, M., Nishihara, Y. and Ha, D. Stripe structure in the CuO_2 plane of perovskite superconductors. *Phys. Rev.*, 1996, **B54**, 12018–12021.
15. Tranquada, J. M. Stripe correlations of spins and holes in cuprate superconductors. *J. Supercond.*, 1997, **10**, 397–399.
16. Bianconi, A., Valletta, A., Perali, A. and Saini, N. L. Superconductivity of a striped phase at the atomic limit. *Physica C*, 1998, **296**, 269–280.
17. Caprara, S., Di Castro, C., Grilli, M., Perali, A. and Sulpizi, M. Fermi surface and gap parameters in high- T_c superconductors: the stripe quantum critical point. *Physica C*, 1999, **317–318**, 230–233.
18. Service, R. F. Could charge stripes be a key to superconductivity? *Science*, 1999, **283**, 1106–1108.
19. Plakida, N. *High-Temperature Superconductivity*. Springer, Berlin, 1995.

20. Kresin, V. Z. and Wolf, S. A. *Fundamentals of Superconductivity*. Plenum Pr., New York, 1992.
21. Kristoffel, N., Konsin, P. and Örd, T. Two-band model for high-temperature superconductivity. *Riv. Nuovo Cimento*, 1994, **17**, 1–41.
22. Konsin, P., Kristoffel, N. and Örd, T. On the composition dependent isotope effect of HTSC in the two-band model. *Ann. Phys.*, 1993, **2**, 279–283.
23. Konsin, P., Kristoffel, N. and Rubin, P. Dependences of superconducting gaps on temperature and carrier concentration in a two-band model. *Solid State Commun.*, 1996, **97**, 567–572.
24. Konsin, P., Kristoffel, N. and Rubin, P. S+D symmetry order parameters in interband superconductivity. *phys. stat. sol. (b)*, 1998, **208**, 145–150.
25. Konsin, P., Kristoffel, N. and Sorkin, B. Application of the interband model to the dependence of superconducting T_c on carrier concentration. *J. Phys.: Condens. Matter.*, 1998, **10**, 6533–6539.
26. Örd, T. and Kristoffel, N. Paired carrier effective mass isotope effect in the two-band model. *phys. stat. sol. (b)*, 1999, **216**, 1049–1056.
27. Kristoffel, N. Description of two-component high- T_c superconductors by an interband model. *phys. stat. sol. (b)*, 1998, **210**, 195–198.
28. Bill, A., Kresin, V. Z. and Wolf, S. A. Isotope effect for the penetration depth in superconductors. *Phys. Rev.*, 1998, **57**, 10814–10824.
29. Örd, T. and Kristoffel, N. Two relaxation times and the high- T_c superconductivity two-component scenario. *Physica C*, 2000, **331**, 13–17.
30. De Wilde, Y., Miyakawa, N., Guptasarma, P., Iavarone, M., Ozyuzer, L., Zasadzinski, J. F., Romano, P., Hinks, D. G., Kendziora, C., Crabtree, G. W. and Gray, K. E. Unusual strong-coupling effects in the tunneling spectroscopy of optimally doped $\text{Bi}_2\text{Sr}_2\text{CaCu}_2\text{O}_{8+\delta}$. *Phys. Rev. Lett.*, 1998, **80**, 153–156.
31. Miyakawa, N., Guptasarma, P., Zasadzinski, J. F., Hinks, D. G. and Gray, K. E. Strong dependence of the superconducting gap on oxygen doping from tunneling measurements. *Phys. Rev. Lett.*, 1998, **80**, 157–160.
32. Miyakawa, N., Zasadzinski, J. F., Ozyuzer, L., Guptasarma, P., Hinks, D. G., Kendziora, C. and Gray, K. E. Predominantly superconductive origin of large energy gaps in underdoped $\text{Bi}_2\text{Sr}_2\text{CaCu}_2\text{O}_{8+\delta}$. *Phys. Rev. Lett.*, 1999, **83**, 1018–1021.
33. Renner, Ch., Revaz, B., Genoud, J.-Y., Kadawaki, K. and Fischer, O. Pseudogap precursor of the superconductivity gap in under- and overdoped $\text{Bi}_2\text{Sr}_2\text{CaCu}_2\text{O}_{8+\delta}$. *Phys. Rev. Lett.*, 1998, **80**, 149–152.
34. Timusk, T. and Statt, B. The pseudogap in high temperature superconductors: an experimental survey. *Rep. Progr. Phys.*, 1999, **62**, 61–115.
35. Timusk, T. Infrared properties of exotic superconductors. *Physica C*, 1999, **317–318**, 18–29.
36. Norman, M. R., Ding, H., Campuzano, J. C., Takeuchi, T., Randeira, M., Yokoya, T., Takahashi, T., Mochiku, T. and Kadowaki, K. Unusual dispersion and line shape of the superconducting state spectra. *Phys. Rev. Lett.*, 1997, **78**, 2628–2631.
37. Kee, H.-Y. and Varma, C. M. Modeling of tunneling spectroscopy in high- T_c superconductors. *Phys. Rev.*, 1998, **B58**, 15035–15044.
38. Yusof, Z., Zasadzinski, J. F., Coffey, C. and Miyakawa, N. Spectral function of superconducting cuprates near optimal doping. *Phys. Rev.*, 1998, **B58**, 514–521.
39. Chubukov, A. V. and Morr, D. K. Density of states and the energy gap in superconducting cuprates. *Phys. Rev. Lett.*, 1998, **81**, 4716–4719.
40. Adrian, S. D., Wolf, S. A., Dolgov, O., Shulga, S. and Kresin, V. Z. Polarizability and single-particle spectra of two-dimensional superconductors. *Phys. Rev.*, 1997, **B56**, 7878–7881.

41. Sherman, A. and Schreiber, M. Spectral and magnetic properties of the two-dimensional t-J mode in the quantum disordered regime. *Physica C*, 1998, **303**, 257–272.

**KÕRGTEMPERATUURSETE ÜLIJUHTIDE OMADUSED
DOPEERIMISEST SÕLTUVA ELEKTRONSPEKTRIGA
KAHETSOONILISES MUDELIS**

Nikolai KRISTOFFEL ja Pavel RUBIN

On käsitletud tsoonidevahelise paariülekandega mudelit põhiaine ja dopeeringuga sündival tsoonil (konstantne seisundite koguarv) kirjeldamiseks kõrgtemperatuurse ülijuhtivuse kahekomponendilist stsenaariumi. On arvatud siirde-temperatuuri, isotoopefekti eksponendi ja ülijuhtivuspilude sõltuvus dopeerimisest teooria parameetrite iseloomulikel väärtustel ja saadud aukdopeeringu kasvuga kahanevad pilude suhted siirde-temperatuuri. Üheosakeselises ergastusspektris on identifitseeritav piik–auk–käär-tüüpi kompleks. Vaatamata jämedatele lähendus-tele peegeldab mudel kupraatülijuhtidel leitud omadusi. Dopeeringust sõltuva elektronspektriga kahetsoonilised mudelid säilitavad koha kõrgtemperatuurse ülijuhtivuse mikromehhanismi tuvastamisel.